On the Separation of Nonadditive Symmetric Mixtures in Nanoscopic Slitlike Pores: A Simple Model for Racemic Fluids

A. Patrykiejew,*,† S. Sokołowski,† and O. Pizio‡

Faculty of Chemistry, MCS University, 20031 Lublin, Poland, and Instituto di Quimica, UNAM, Mexico City, Mexico

Received: April 27, 2004; In Final Form: January 21, 2005

A grand canonical ensemble Monte Carlo simulation method is used to study the adsorption of nonadditive symmetric mixtures of Lennard−Jones spherical particles in nanoscopic slitlike pores. The walls of the pore are assumed to be formed by the parallel (100) planes of the model face centered cubic crystal of adjustable corrugation potential. It is demonstrated that depending on the nonadditivity effects in the mixture and the pore width the condensed phases formed inside the pore may have different structures. In particular, it is shown that the mixture may separate into layers containing only one component each and the stacking may depend on the pore width and properties of the mixture.

1. Introduction

One of the very important problems in chemistry, biology, but probably most of all in medicine is the separation of racemic mixtures,[1−6] which consist of the *R* and *S*[7] isomers, and usually have different biological effects. Thalidomide is, probably, the best known and tragic example that shows how important a good separation of *R* and *S* enantiomers can be.[8,9]

The thermodynamic properties of racemic liquid mixtures are usually very similar to the properties of their pure components,[10,11] and hence such mixtures cannot be separated by conventional methods, such as distillation. Nevertheless, separation of racemic mixtures can be achieved in a number of ways,[1−6] and many of them involve adsorption. It became clear already at the end of 19th century[4] that upon crystallization racemic mixtures may form different solid phases and, in particular, may separate into *R* and *S* crystals. Chromatographic methods of enantiomer separation[6] are based on the observation that the *R* and *S* isomers interact differently with a chiral chromatographic phase.[5] Over the past 20 years, the number of chiral stationary phases has become available and used in enantioselective gas[12,13] and liquid[14] chromatography. The enantoselectivity of chiral stationary phases is often relatively low and various recycling techniques, such as steady-state recycling[15] and simulated moving bed,[16] are used.

The difference between enantiomeric molecules is purely geometrical because of the lack of a rotation-inversion axis, and induces steric effects that cause the interaction potentials for the like−like (*R*−*R* and *S*−*S*) and like−unlike (*R*−*S*) pairs of molecules to be different.[17−19] Although real racemic mixtures consist of rather complex multiatomic molecules, such as 1,2-*trans*-dimethylcyclopropan, one can capture their most important qualitative properties by using a simple model of atomic nonadditive symmetric mixture.[20,21] This model has been applied already to study the bulk properties of racemic liquid mixtures.[20]

Thermodynamic and structural properties of symmetric binary mixtures have been studied by several authors.[22−26] Those studies concentrated on the understanding of the phase behavior of uniform as well as nonuniform systems. It has been demonstrated[25] that depending on the nonadditivity effects, different topologies of phase diagrams appear in the bulk. In particular, demixing transition may start at the critical end point or at the tricritical point. In the case of nonuniform systems, that is, when the mixture is a subject of external potential resulting from the presence of adsorbing walls, competing effects of fluid−fluid and fluid−wall interactions lead to a particularly rich phase behavior.[27−29] In general, in all of those studies the nonadditivity effects have been assumed to be rather strong and hence the demixing transition was observed in liquid phases. It is not a case for typical racemic mixtures, which exhibit weak nonadditivity effects and hence their separation may occur only via crystallization or chromatography. Computer simulations, performed by Vlot et al.,[20] for nonadditive Lennard−Jones symmetric mixtures characterized by different size and energy nonadditivity effects demonstrated that when the interaction energy between like−unlike pairs of molecules becomes low enough, the phase separation occurs already in a liquid state, just the same as that observed by other authors.[22,24] The presence of external fields may significantly enhance a tendency of a mixture to separate into *R*-rich and *S*-rich phases. In particular, one can expect that adsorption at crystalline walls of appropriately chosen lattice symmetry and corrugation of the surface potential should lead to the phase separation when the nonadditivity effects are weaker than necessary to separate bulk mixtures. In such systems, the adsorbed layers show considerably higher ordering than the uniform (bulk) phases, and hence are more likely to form solidlike structures. In fact, the possibility of racemic mixture separation in monolayer films formed at different faces of metal crystals has been discussed by Sholl and co-workers.[30−32] In their works they used a rather complex, multiatomic model of enantiomers. Another interesting model that may be used in computer simulation studies of racemic mixtures is that based on the Gay−Berne potential,[33] quite successfully used by Memmer[34,35] to investigate the properties of chiral liquid crystals. However, a possibility of achieving separation of racemic mixtures, modeled as a mixture of spherical particles with nonadditive interactions, adsorbed

* Corresponding author. E-mail: andrzej@miki.umcs.lublin.pl.
† MCS University.
‡ Instituto di Quimica.

10.1021/jp048170b CCC: $30.25
Published on Web 07/01/2005

at crystalline surfaces and in slitlike pores with crystalline walls has not been explored yet.

In this paper we present the results of a Monte Carlo study demonstrating that a simple nonadditive symmetric Lennard−Jones mixture can be separated when adsorbed in slitlike micropores. One should note that we have not attempted to perform any systematic studies, but we have attempted to show that the geometrical confinement, nonadditivity effects, as well as the properties of the surface potential all have a considerable influence on the structure of condensed phases formed under confinement and give examples of conditions under which such simple model racemic mixtures can be separated.

2. Model and Methods

As was already mentioned in the Introduction, we consider a very simple model of a nonadditive binary symmetric mixture,[20] which consists of spherical particles interacting via the isotropic Lennard−Jones potential

$$u(r) = \begin{cases} 4\epsilon_{i,j}[(\sigma_{i,j}/r)^{12} - (\sigma_{i,j}/r)^{6}] & r \le r_{\max} \\ 0 & r > r_{\max} \end{cases} \qquad (1)$$

where i and j refer to the components of the mixture (1 and 2) and r is the distance between the interacting particles. Because the mixture is symmetric, $\epsilon_{1,1} = \epsilon_{2,2} = \epsilon$, $\sigma_{1,1} = \sigma_{2,2} = \sigma$. For the like−unlike pairs, we assume that $\epsilon_{1,2} = \epsilon_{2,1} = e\epsilon$, $\sigma_{1,2} = \sigma_{2,1} = s\sigma$. Parameters e and s, which can be lesser as well as greater than unity, define the effects of nonadditivity and mimic steric and energetic effects pertinent to racemic mixtures. In fact, the above model is the same as that used by Vlot et al.[20] in their study of bulk racemic mixtures.

Then we assume that such a mixture is placed in a slitlike pore of the walls formed by the (100) face of a model fcc crystal. The potential representing the interaction between a fluid atom and a single wall can be written as[36]

$$v^*(z^*, \tau^*) = \epsilon^*_{gs}[v_o(z^*) + V_b \sum_{g\neq 0} v_g(z^*) f_g(\tau^*)] \qquad (2)$$

In the above expression, $\tau^* = (x^*, y^*)$ ($x^* = x/a$, $y^* = y/a$) is the 2D vector that specifies the position of an adatom over the surface plane, the sum runs over all of the nonzero reciprocal lattice vectors of the length, g, and $z^* = z/a$ is the distance from the surface. The parameter $\epsilon^*_{gs} = \epsilon_{gs}/\epsilon$ measures the strength of the interaction between a fluid atom and a single atom of the solid, and V_b controls the corrugation part of the potential.[37] The Fourier components $v_o(z)$ and $v_g(z)$ as well as the functions $f_g(\tau)$ can be found in ref 36. Note that in our special case of a symmetric mixture, both components interact the same with the surface, and hence we have dropped the component indices in the above eq 2. Assuming next that there is no phase shift between the pore walls, that is, the unit cells of both walls have the same relative positions, the interaction of a fluid particle with the pore walls is the sum of interactions with individual walls and is given by

$$V^*_p(z^*, \tau^*) = v^*(z^*, \tau^*) + v^*(H^* - z^*, \tau^*) \qquad (3)$$

where $H^* = H/a$ is the pore width. In this work, we concentrate on a class of systems in which the pore width $H^* = H/a$ changes between $H^* = 3.0$ and 8.0 and fix the size of the adsorbate atoms $\sigma^* = \sigma/a = 1.0$. Parameters e and s are varied and we assume that e is equal to or lower than 1.0, whereas s is varied between 1.2 and 1.5. The values of e not exceeding 1.0 and s well above 1.0 cause the bulk, as well as the confined condensed phases, to have a natural tendency to phase separation at sufficiently low temperatures.[20] Of course, in real racemic mixtures the interaction between like−like and like−unlike pairs may lead to the effective potentials characterized by e higher than 1.0 and/or s lower than 1.0.

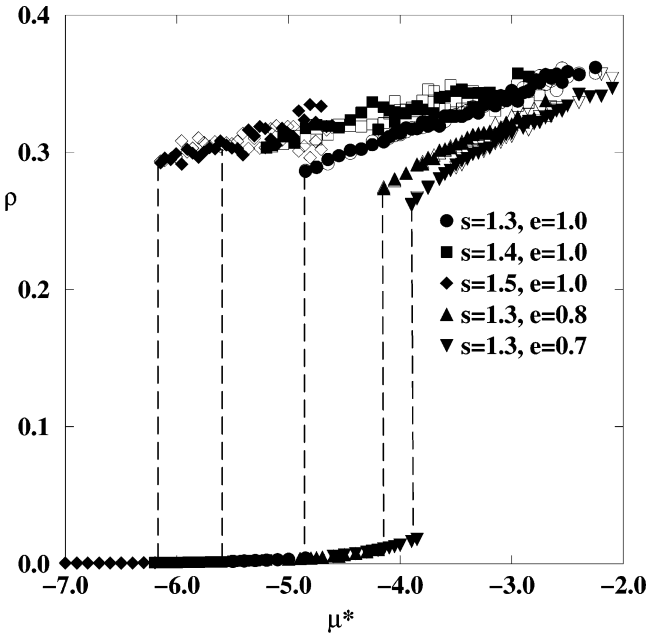

Figure 1. Isotherms, at $T^* = 0.9$, for bulk systems characterized by different values of parameters s and e (shown in the figure). The same open and filled symbols mark the densities of different components.

We use a standard Monte Carlo method in the grand canonical ensemble,[38,39] which was used successfully to study one-component fluids adsorbed in pores with crystalline walls.[40] All of the calculations have been performed assuming that the size of the simulation box in x and y directions was equal to $L^*_x = L^*_y = 20$, with periodic boundary conditions applied in both x and y directions. In the z direction, the size of the system is determined by the pore width. Each Monte Carlo step consisted of attempts to displace a randomly chosen particle in the system by, also randomly chosen, a 3D vector from the cube of the side $d_{\max}$, annihilation of a randomly chosen particle, creation of a particle, of either component 1 or 2, at a randomly chosen position, and a change of identity of a randomly chosen particle. Because racemic mixtures are equimolar, the chemical potentials of both species are bound to be the same. It allows one to use only a single variable, $\mu^* = \mu/\epsilon$, which controls the chemical potentials of the components. The number of Monte Carlo steps ranged between $10^6 N_t$ and $5 \times 10^6 N_t$, where N_t is the number of particles in the system at any given instance of simulation.

3. Results and Discussion

We begin with the presentation of some selected results, which illustrate the behavior of bulk systems. Because the majority of our calculations has been carried out at a fixed temperature, $T^* = 0.9$, which is lower than the bulk critical temperatures of all of the systems considered, we concentrate on that case. Figure 1 presents the examples of isotherms obtained for the systems characterized by different values of nonadditivity parameters e and s, which show that the condensed (liquid) phases remain well mixed. Also, all of these isotherms exhibit density jumps, indicating the first-order condensation transition.

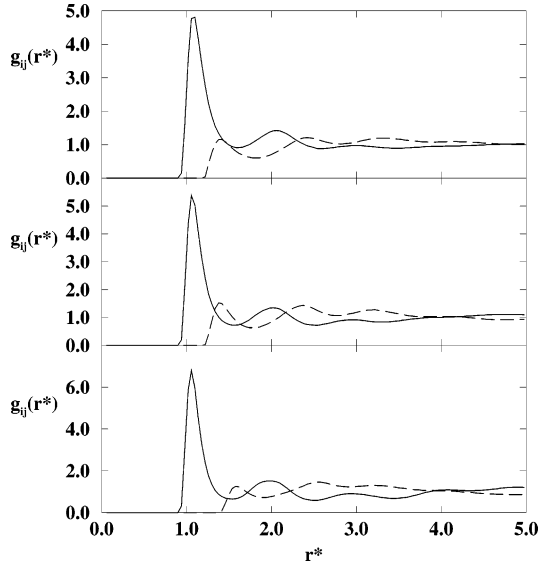

Figure 2. Radial distribution functions, $g_{11}(r)$ (solid lines) and $g_{12}(r)$ (dashed lines), obtained for the bulk systems characterized by $e = 0.7$ and $s = 1.3$ (upper panel), $e = 1.0$ and $s = 1.3$ (middle panel), and $e = 1.0$ and $s = 1.5$ (bottom panel) at the temperature $T^* = 0.9$ and the chemical potential $\mu^* = -3.0$.

We have also calculated the composition of the liquid phase in small blocks, obtained by dividing the entire system of the size $20 \times 20 \times 20$ into cells of the size $5 \times 5 \times 5$, to check whether regions of nonuniform distribution of components exist, but the results have clearly demonstrated that over the range of chemical potentials used here, the liquid phase remains uniform. The examples of the radial distribution functions, given in Figure 2, also show that the condensed phase is a liquid. Note that the shifts in the positions of the maxima of $g_{12}(r)$, with respect to the corresponding maxima of $g_{ii}(r)$ ($i = 1, 2$), result from the nonadditivity effects.

Of course, when the effects due to nonadditivity become large enough, one expects to observe a demixing transition at sufficiently high densities, that is, at sufficiently high values of the chemical potential. Similarly, a phase separation should occur when the temperature is decreased. Indeed, the isotherms obtained for the system with $s = 1.4$ and $e = 1.0$ at a temperature of $T^* = 0.70$ and lower, demonstrate that the condensed liquid phase is partially demixed. For the sake of brevity, we do not present the relevant figures. One can expect that within the range of nonadditivity parameters used here, the bulk phase diagrams should belong to the third class according to the classification introduced by Wilding et al.,[25] that is, for an equimolar gaseous mixture the phase diagram exhibits a critical end point located well below the critical point of the gas−liquid condensation. The critical end point is onset of the λ-line marking a continuous (higher-order) demixing transition within a condensed phase. Our results shown in Figures 1 and 2 indicated that for the system with $s = 1.4$ and $e = 1.0$, the critical end point is located at a temperature between 0.7 and 0.9. We have not, however, attempted to estimate bulk phase diagrams.

The first series of calculations for our model mixtures in pores have been performed for the systems characterized by the fixed values of $\epsilon^*_{gs} = 1.0$, $V_b = 1.0$ and of the energetic nonadditivity parameter $e = 1.0$. The purpose of our calculations was to demonstrate how the steric effects, measured by the deviations of parameter s from unity, influence the structure of condensed phases formed in the pores of different width and characterized by rather strongly attractive and strongly corrugated surface

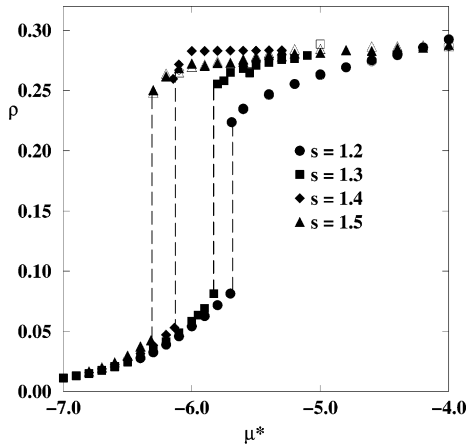

Figure 3. Adsorption isotherms for mixtures with different values of parameter s (shown in the figure) in the pore of $H^* = 6.0$ at $T^* = 0.9$. Open and filled symbols mark the densities of different components.

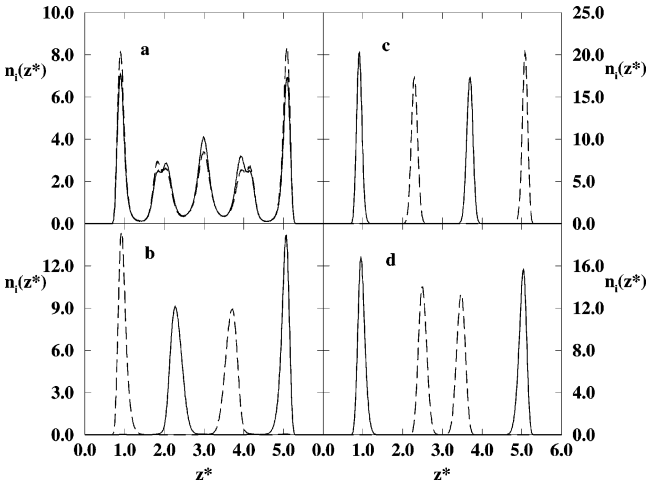

Figure 4. Examples of density profiles for the systems characterized by $H^* = 6.0$ and different values of parameter s equal to 1.2 at $\mu^* = -2.6$ (part a), 1.3 at $\mu^* = -5.2$ (part b), 1.4 at $\mu^* = -5.5$ (part c), and 1.5 at $\mu^* = -5.5$ (part d) obtained at $T^* = 0.9$. Solid and dashed lines are for different components.

potential. For this purpose we have chosen the mixtures, characterized by s varying between 1.2 and 1.5, adsorbed in the pores of H^* ranging from 3.0 to 8.0, in which different numbers of adsorbate layers are formed.

To elucidate the effects of steric effects, we now discuss the properties of a series of mixtures characterized by different values of s, placed in a slitlike pore of the fixed width $H^* = 6.0$. Although we are interested in the behavior of dense, liquidlike phases rather than in a detailed study of condensation due to adsorption from the gaseous phase, we have also evaluated the adsorption isotherms in order to show that the capillary condensation transition occurs at the chemical potentials below the bulk coexistence point (see Figure 3). The isotherms given in Figure 3 also demonstrate that the condensed phase does not exhibit a demixing transition so that in all cases the densities of both components are practically the same along the isotherms, although it is possible that demixing may occur at higher values of the chemical potential. The observed perfect mixing of the dense phases does not mean, however, that their structures in confined geometry are the same.

The density profiles obtained for the systems characterized by different values of parameter s are compared in Figure 4 and clearly demonstrate that the structure of the condensed phase depends quite strongly on the magnitude of parameter s. Thus,

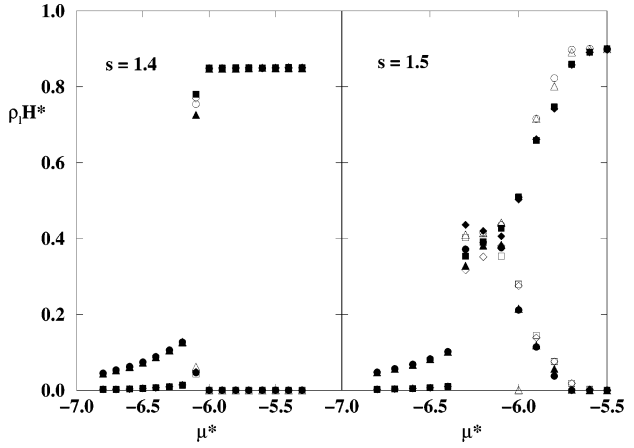

Figure 5. Changes of layer densities with the chemical potential for the systems characterized by $H^* = 6.0$ and $s = 1.4$ and 1.5 at $T^* = 0.9$. Open and filled symbols mark the densities of different components and different symbols correspond to the densities in different layers: Circles − layer 1, squares − layer 2, diamonds − layer 3, triangles − layer 4.

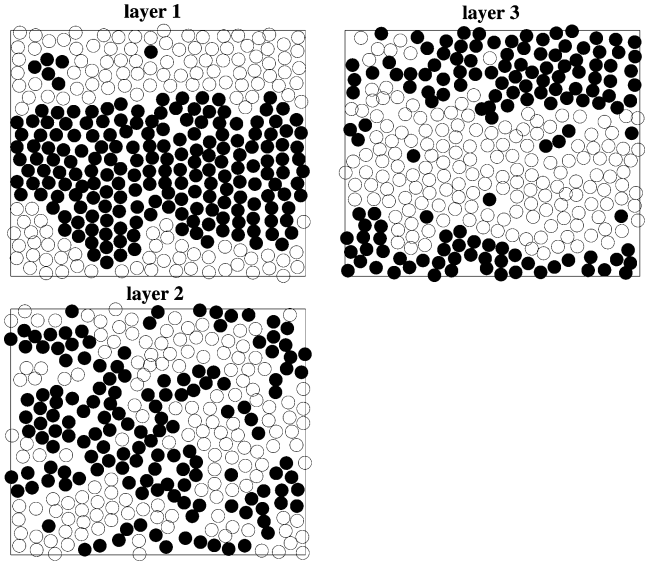

Figure 6. $x-y$ projections of the configuration of the first three layers obtained for the system with $H^* = 6.0$, $s = 1.2$ at $T^* = 0.9$, and $\mu^* = -2.60$. Open and filled circles mark the particles of component 1 and 2, respectively.

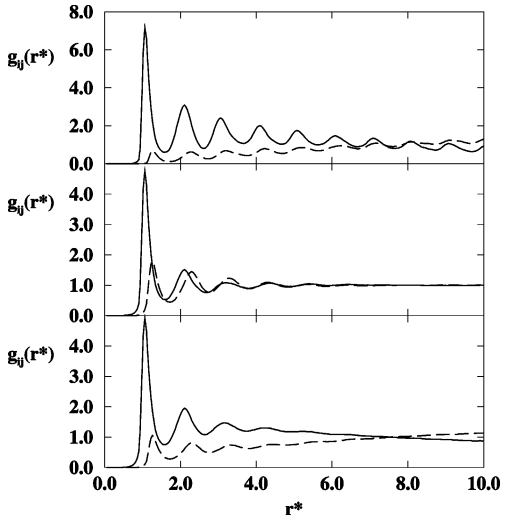

Figure 7. Radial distribution functions, $g_{11}(r)$ (solid lines) and $g_{12}(r)$ (dashed lines), in the first (upper panel), second (middle panel), and third (bottom panel) layer, for the system with $H^* = 6.0$, $s = 1.2$ at $T^* = 0.9$, and $\mu^* = -2.60$.

when $s = 1.2$ the adsorbate forms five mixed layers, whereas for $s = 1.3$, 1.4, and 1.5 the condensed phase consists of only four layers and each of them contains only one component. In the case of $s = 1.3$ and 1.4 the stacking of layers is 1212, which means that layers 1 and 3 contain only the component 1 and layers 2 and 4 contain only the second component, whereas in the case of $s = 1.5$ we obtain a different sequence of layers in which one component is concentrated in the layers adjacent to the pore walls (contact layers) and the other component occupies middle layers only (1221 stacking). The distance of the contact layers from the surface increases slightly when parameter s increases, for example, for $s = 1.2$ the corresponding maxima at the local density profile occur at the distance from the surface equal to about 0.9, whereas for $s = 1.5$ those maxima are located at about 0.95. The changes in the number of adsorbate layers as well as their stacking result from the changes of steric parameter s. In the case of $s = 1.3$ and 1.4, the interlayer distances are slightly lower than $s2^{1/6}$, which corresponds to the location of the minimum of the LJ potential between unlike particles. The same holds for the distance between the contact and the middle layers when $s = 1.5$. However,in the latter system, the distance between the two middle layers, consisting of the same component, is slightly lower than 1.0, that is, it is lower than $2^{1/6}$ but nearly equal to the interparticle distance in the body centered cubic lattice ($2^{1/6}\sqrt{3}/2 \approx 0.97$). Parts b and c of Figure 4 also demonstrate that the increase of nonadditivity parameter s leads to a higher localization of all layers so that the local density peaks become narrower.

The separation of the mixture into 1-rich and 2-rich layers occurs either right at the adsorbate condensation point or starts at the values of the chemical potential above the condensation point and gradually develops upon the increase of the chemical potential, that is, upon the increase of the density. Both situations are illustrated in Figure 5, which presents the changes of layer densities with μ^* obtained for the systems characterized by $s = 1.4$ and 1.5. The observed different behavior is likely to be connected with the changes of the packing effects, which also result in the evolution of the layer stacking. The inspection of configurations recorded during Monte Carlo runs, not shown here, confirms that for $s = 1.5$ and the chemical potential around -6.2 the layers remain mixed.

The above-presented density profile obtained for the system with $s = 1.2$ shows that the confined condensed phase does not separate into 1-rich and 2-rich layers. However, the inspection of configurations allows us to conclude that such a separation does take place within each layer. Figure 6 shows the x, y projection of the configurations of the first three layers recorded at rather high value of the chemical potential equal to $\mu^* = -2.6$. These configurations demonstrate that the contact layer consists of two large uniaxially ordered domains containing one component each, whereas the separation in liquidlike layers 2 and 3 is only partial. Radial distribution functions (see Figure 7) also demonstrate that the contact layers are highly ordered, whereas the middle layers are liquidlike. The structure in layers 4 and 5 is very much the same as that in layers 2 and 1, respectively. Our results suggest that the melting in the pore is anisotropic, and it occurs at lower temperatures in the middle layers than in the contact layers. The above statement is well supported by the snapshots and the radial distribution functions. A stronger effect of separation in the central layer as compared with layer 2 (and 4) can be attributed to the specific packing effects for the system discussed here.

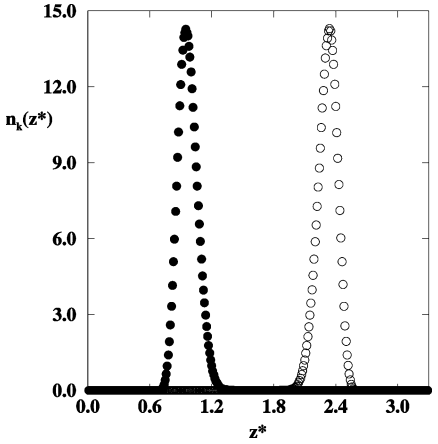

Figure 8. Density profiles obtained for the systems characterized by $s = 1.3$, $e = 1.0$, and $H^* = 3.3$ at $T^* = 0.9$ and $\mu^* = -6.60$. Open and filled circles correspond to different components.

Of course, one expects that the structure of condensed phases and, in particular, the separation into 1-rich and 2-rich domains within layers or into 1-rich and 2-rich layers should depend strongly on the pore width. Already the above shown difference in the structure of condensed phases for the systems characterized by $s = 1.4$ and 1.5 demonstrates that even small changes in the system geometry may influence its properties considerably. Those changes are driven by the packing effects, which are expected to be rather sensitive to the pore width. Here, we concentrate on the mixtures characterized by different values of parameter s adsorbed in pores of the width ranging from 3.0 to 8.0.

In the case of very narrow pores, for example, of $H^* = 3.0$ and 3.4, in which only two atomic layers appear, we have found that for s ranging from 1.2 to 1.5, the condensed phase separates into 1-rich and 2-rich layers (see Figure 8). Upon the increase of H^*, the regime of three-layer structures is reached. The threshold value of the pore width (H^*_{2-3}), which separates the two-layer and three-layer regimes, depends on the value of parameter s, though we have not attempted to make any quantitative estimations of H^*_{2-3}. In the case of $H^* = 4.0$, three layers, equally populated by both components, have been found for all systems studied, that is, for $s = 1.3$, 1.4, and 1.5. The recorded configurations (Figure 9) indicate that each layer has axially ordered structures, consisting of long chainlike aggregates built of different components and oriented along one of the symmetry axes. One should note that the chains of the same component are located atop one another across the entire pore. The thickness of those chains changes with s, and we have found that it decreases with the increase of s.

The results obtained for $H^* = 5.0$ and the mixtures characterized by $s = 1.4$ and 1.5 demonstrate different behavior and also illustrate the above-mentioned dependence of the threshold value of H^*, which separates different regimes, on the magnitude of nonadditivity parameter s. In the case of $s = 1.5$, we still observe the formation of three layers, but now the structure of the condensed phase is quite different than that in the case of $H^* = 4.0$, and the mixture separates into 1-rich and 2-rich layers.

Figure 10a presents the density profile recorded at $T^* = 0.9$ and $\mu^* = -6.0$, showing that both contact layers are occupied by one component, whereas the second component occupies only the middle layer. In this case we observe that the average density of one component in the entire pore is more than twice the density of the second component. Thus, the confinement leads to a partial segregation of the mixture as illustrated in Figure 10b. This figure also shows that the condensed demixed

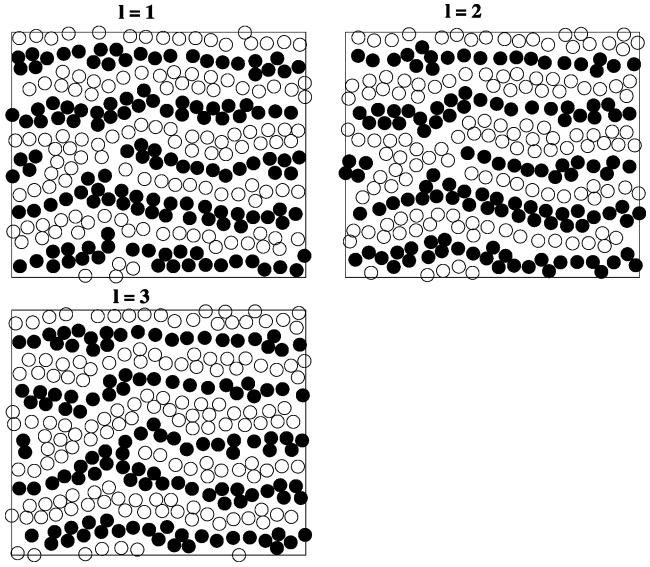

Figure 9. $x-y$ projections of the layer configurations recorded for the system with $H^* = 4.0$ and $s = 1.4$ at $T^* = 0.9$ and $\mu^* = -4.20$. Open and filled circles mark particles of component 1 and 2, respectively.

phase fluctuates beteen two states with the interchanged densities of both components. We recall that under the same thermodynamic conditions the bulk liquid is an equimolar mixture of both components. However, when $s = 1.4$ the structure of the condensed phase seems to be different and the density profiles show the presence of five maxima and lack of separation into 1-rich and 2-rich layers. The contact and middle layers are much more highly populated than layers 2 and 4. The configuration depicted in Figure 11 demonstrates that in each layer the domains consisting of different components are present. This figure also shows that the particles in layers 2 and 4 occupy only the regions at the boundaries of domains containing different components in layers 1, 3, and 5.

In the already discussed case of $H^* = 6.0$, the number of layers may be five ($s = 1.2$) or four ($s = 1.3$, 1.4 and 1.5) and the structure of condensed phases also changes with s.

For still wider pores of $H^* = 7.0$ and 8.0, the structure of adsorbed condensed phases becomes more complex. The number of atomic layers increases and, depending on the choice of s, different stacking of 1-rich and 2-rich layers occurs. For example, for $s = 1.5$ and $H^* = 8.0$ (Figure 12a) as well as for $s = 1.4$ and $H^* = 7.0$ (Figure 12b) we find a similar six-layer structure of the stacking 122112. However, in the case of $s = 1.4$ and $H^* = 7.0$ the middle layers are not as well separated as those in the case of $s = 1.5$ and $H^* = 8.0$

All of the above-presented results have been obtained for the systems characterized by rather strongly attractive ($\epsilon^*_{gs} = 1.0$) and strongly corrugated ($V_b = 1.0$) surface potential. In particular, the energy of adsorption has been considerably higher than the fluid−fluid interaction energy and the potential barriers for translation have been of a magnitude exceeding ϵ. One can expect that in the pores characterized by weaker as well as by less corrugated surface fields the structure of the condensed phases changes. Our preliminary results demonstrate, however, that it is the confinement, that is, the pore width, rather than the properties of the fluid-wall potential that determines the structure and a possible separation of the mixture. It is so because in the case of nonadditive mixtures with strong steric effects the packing and stacking of adsorbed particles is dominated by the geometry of the system. For example, Figure 13 shows the examples of density profiles obtained for the

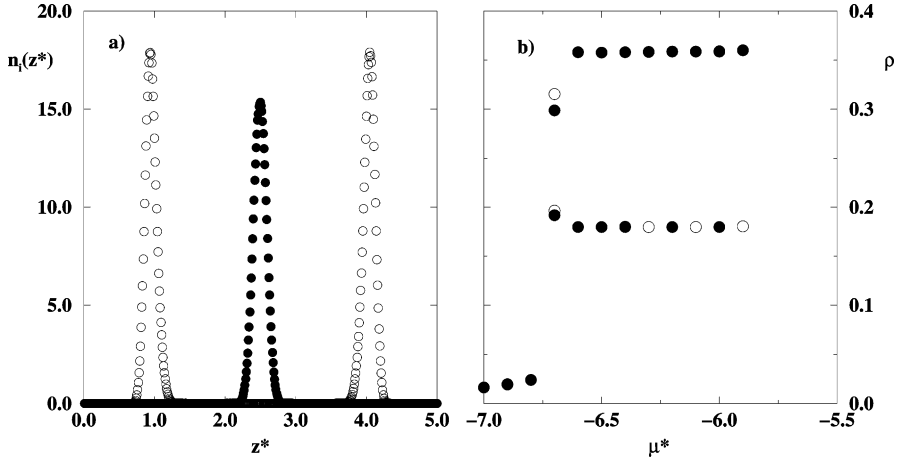

Figure 10. (Part a) Density profile obtained for the system characterized by $s = 1.5$, $e = 1.0$, and $H^* = 5.0$ recorded at $T^* = 0.9$ and $\mu^* = -6.0$. Open and filled circles correspond to different components. (Part b) Adsorption isotherm for the same system at $T^* = 0.9$. Open and filled circles correspond to different components.

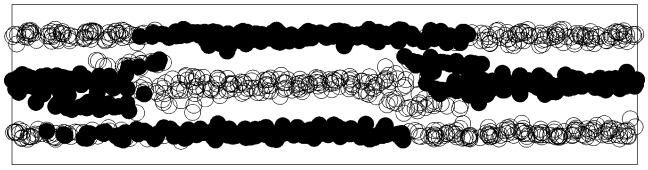

Figure 11. $x-z$ projection of the configuration obtained for the system with $H^* = 5.0$ and $s = 1.4$ at $T^* = 0.9$ and $\mu^* = -3.60$. Open and filled circles mark particles of component 1 and 2, respectively.

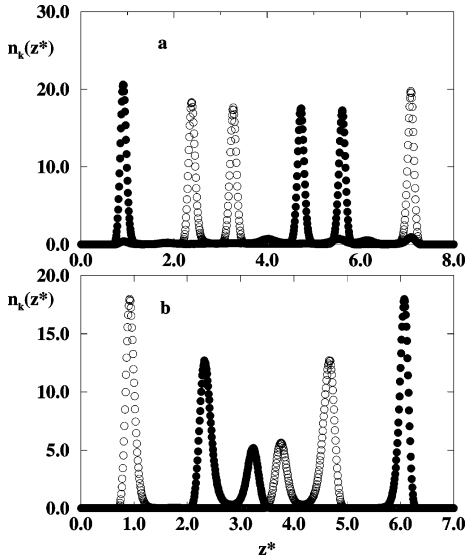

Figure 12. Density profiles obtained for the system characterized by $s = 1.5$, $e = 1.0$, and $H^* = 8.0$ (part a) and $s = 1.4$, $e = 1.0$, and $H^* = 7.0$ (part b) recorded at $T^* = 0.9$ and $\mu^* = -5.2$. Open and filled circles correspond to different components.

systems with $H^* = 6.0$, $s = 1.3$, and $e = 1.0$ but characterized by different corrugation of the surface potential, measured by parameter V_b. It is quite evident that the structure of the condensed phase remains the same independent of V_b. The middle panel of Figure 13, which presents the results obtained for $V_b = 0.5$, shows that the separation is not complete, but it becomes complete at still higher values of the chemical potential so that the density profile becomes the same as that in the lower and upper panels of Figure 13.

Nonadditivity effects are also connected with the deviations of parameter e from unity. We have performed the calculations for the model mixtures characterized by $s = 1.3$ and by different values of e equal to 0.7, 0.8, 0.9, and 1.0, adsorbed in the pore

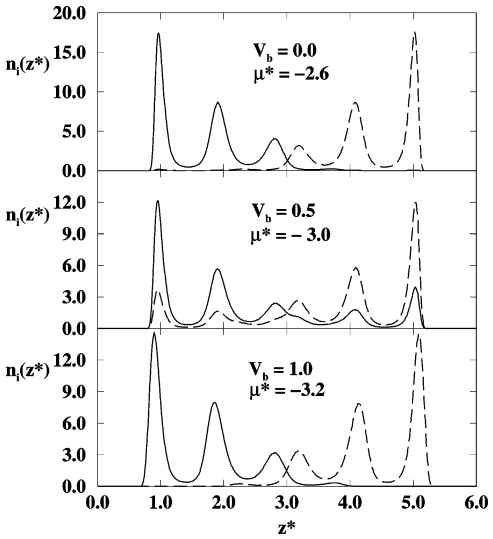

Figure 13. Density profiles, obtained at $T^* = 0.9$, and the chemical potentials shown in the figure for the systems characterized by $H^* = 6.0$, $s = 1.3$, $e = 1.0$, and the surface potential with $\epsilon^*_{gs} = 1.0$ but of different corrugation (measured by parameter V_b). Solid and dashed lines correspond to different components.

of the fixed width equal to $H^* = 6$. The system characterized by $e = 1.0$ is used here as a reference, and its properties are illustrated in Figure 14a, which shows the density profile obtained at $\mu^* = 4.6$. The remaining parts of Figure 14 show the density profiles for the systems characterized by different values of $e = 0.9$, 0.8, and 0.7. One readily notes that the changes in e affect the structure of the condensed phase considerably. Lowering of e from 1.0 to 0.9 results in the formation of 1-rich and 2-rich small droplets in the entire pore rather than to the separation into 1-rich and 2-rich layers, and consequently the density profile shows a rather complex structure. A further decrease of e to 0.8 leads to the separation of the mixture into 1-rich contact layers and 2-rich three middle layers. Finally for $e = 0.7$, 1-rich and 2-rich phases are located at different pore walls and the "interface" is located at the pore center.

Taking into account that the ultimate goal of our study is to explore the possibility to use adsorption in pores as a first step leading to the extraction of both enantiomers in a pure form, the above-presented results seem to be quite interesting and promissing. The formation of layer structures with only one component in each layer shows that a confinement-driven

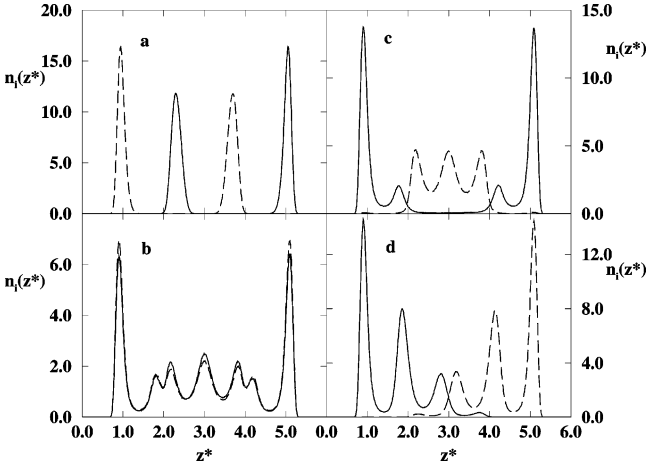

Figure 14. Density profiles, obtained at $T^* = 0.9$, for the systems characterized by $H^* = 6.0$, $s = 1.3$, and different values of parameter $e = 1.0$ at $\mu^* = -4.6$ (part a), $e = 0.9$ at $\mu^* = -3.8$ (part b), $e = 0.8$ at $\mu^* = -3.7$ (part c), and $e = 0.7$ at $\mu^* = -3.2$ (part d). Solid and dashed lines correspond to different components.

separation of nonadditive mixtures does occur. Particularly interesting is the structure in which one component occupies contact layers only, whereas the second component is located in the middle layers as well as any other structures symmetric with respect to the plane parallel to the pore walls and located at the pore center, at $H^*/2$. The above-presented results demonstrate quite well that such structures do occur when the pore width is suitably chosen. Of course, the separation of the mixture inside the pore is only the first step of the process aiming at the extraction of both components in a pure form. Therefore, the means must be found to extract pure components from the pore. This can probably be achieved by one of the following procedures.

The first experimentally feasible method would be to considerably reduce the temperature after the adsorption process has been completed so that the adsorbed phase becomes solidlike. After pumping out the bulk (gaseous) mixture, the temperature should be raised again, in a controlled manner, leading to gradual desorption. If the adsorbate condensed phase is such that both contact layers contain only one component and the surface field is strongly attractive, then the desorption should first involve the particles located close to the pore center (the other component), leaving the contact layers more or less unchanged. In this way it may be possible to obtain fractions enriched with different components.

Another possibility may be to perform the adsorption step and then to admit another adsorbate into the system. Then, upon an increase of pressure, the component occupying the middle layers would be removed gradually. Of course, that additional adsorbate must have very special properties. First of all, its adsorption energy should be considerably lower than the adsorption energy of the racemic mixture. It is important because we want the contact layers to remain unchanged when the pressure of the third component increases. Moreover, the interaction of the third adsorbate with the components of the racemic mixture should fulfill some special conditions. Thus, the size of its particles should be chosen in such a way that it can readily penetrate the pore interior without replacing the molecules located in the contact layers.

We plan to perform appropriate computer simulations in order to see if such methods can lead to the desired results, that is, the extraction of individual components.

To understand fully the behavior of nonadditive mixtures in pores it is very desirable for one to possess a detailed knowledge about the properties of such systems in the ground state ($T^* = 0$). The results of our Monte Carlo simulations show that in some cases the structure of condensed phase exhibits different ordering from run to run, and it is not clear which of them represents a true equilibrium structure and which is metastable.

Of course, the model used here is far too simple to capture the properties of real racemic mixtures. Nonadditive Lennard−Jones mixtures contain spherical particles and hence do not possess the properties that allow one to properly take into account the differences between the interactions of enantiomers. The specific symmetry properties of enantiomers, which are mirror images, cannot be mapped onto the steric as well as energetic parameters, which enter our model. Besides, the interaction of nonspherical molecules with the pore walls is bound to be strongly orientation-dependent, whereas our model completely ignores such effects.

Nevertheless, we believe that the steric and energetic effects, which also appear in real racemic mixtures, may be a driving force enabling separation of enantiomers in slitlike pores with walls with appropriate properties of the surface potential and with suitably chosen pore width.

Acknowledgment. This work has been supported by CONACyT under grant no. 37323-E and by European Community under grant MTKD-CT-2004-509249.

References and Notes

(1) Jacques, J.; Collet, A.; Wilen, S. H. *Enantiomers, Racemates, and Resolutions*; Krieger: Melbourne, FL, 1991.
(2) Armstrong, D. W.; Tang, Y.; Ward, T. *Anal. Chem.* **1993**, *65*, 1114.
(3) Armstrong, D. W.; Tang, Y.; Chen, S. *Anal. Chem.* **1994**, *66*, 1473.
(4) Roozenboom, H. W. B. *Z. Phys. Chem.* **1899**, *28*, 494.
(5) Pirkle, W. H.; Pochapsky, T. C. *Chem. Rev.* **1989**, *89*, 347.
(6) Guebitz, G. *Chromatographia* **1990**, *30*, 555.
(7) Morrison, R. T.; Byod, R. N. *Organic Chemistry*; Allyn and Bacon: Boston, MA, 1987.
(8) Muller, G. W.; Konnecke, W. E.; Smith, A. M.; Khetani, V. D. *Org. Process Res. Dev.* **1999**, *3*, 139.
(9) Tekeuchi, Y.; Shiragami, T.; Kimura, K.; Suzuki, E.; Shibata, N. *Org. Lett.* **1999**, *1*, 1571.
(10) Atik, Z.; Ewing, M. B.; McGlashan, M. L. *J. Chem. Thermodyn.* **1983**, *15*, 159.
(11) Lepori, L.; Koppenhoefre, B. *J. Phys. Chem.* **1994**, *98*, 6862.
(12) Schurig, V.; Nowotny, H.-P. *J. Chromatogr.* **1988**, *441*, 155.
(13) Grosenick, H.; Schurig, V. *J. Chromatogr., A* **1997**, *761*, 181.
(14) Miller, L.; Orihuela, C.; Fronek, R.; Murphy, J. *J. Chromatogr., A* **1999**, *865*, 211.
(15) Grill, C. M. *J. Chromatogr., A* **1998**, *796*, 101.
(16) Ruthven, D. M.; Ching, C. B. *Chem. Eng. Sci.* **1989**, *44*, 1011.
(17) Craig, D. P.; Schipper, P. E. *Proc. R. Soc. London, Ser. A* **1975**, *342*, 19.
(18) Craig, D. P.; Thirunamachandran, T. *J. Chem. Phys.* **1998**, *109*, 1259.
(19) Paci, I.; Dunford, J.; Cann, N. M. *J. Chem. Phys.* **2003**, *118*, 7519.
(20) Vlot, M. J.; Claassen, S.; Huitema, H. E. A.; Van der Eerden, J. P. *Mol. Phys.* **1997**, *91*, 19.
(21) Jagennathan, K.; Yethiraj, A. *J. Chem. Phys.* **2003**, *118*, 7907.
(22) Georgoulaki, A.; Ntouros, I. V.; Tassios, D. P.; Panagiotopoulos, A. Z. *Fluid Phase Equilib.* **1994**, *100*, 153.
(23) Hoheisel, C. *Theoretical Treatement of Liquids and Liquid Mixtures, Studies in Physical and Theoretical Chemistry*; Elsevier: Amsterdam, 1993; Vol. 80.
(24) Van Konynenburg, P. H.; Scott, R. L. *Philos. Trans. R. Soc. London, Ser. A* **1980**, *298*, 495.
(25) Wilding, N. B.; Schmid, F.; Nielaba, P. *Phys. Rev. E* **1998**, *58*, 2201.
(26) Góźdź, W. T. *J. Chem. Phys.* **2003**, *119*, 3309.
(27) Dietrich, S.; Schick, M. *Phys. Rev. B* **1985**, *33*, 4952.
(28) Schmid, F.; Wilding, N. B. *Phys. Rev. E* **2001**, *63*, 031201.
(29) Bucior, K.; Patrykiejew, A.; Pizio, O.; Sokołowski, S. *Mol. Phys.* **101**, *721*, 2003.
(30) Sholl, D. S. *Langmuir* **1998**, *14*, 862.
(31) Power, D. P.; Sholl, D. S. *J. Vac. Sci. Technol., A* **1999**, *17*, 1700.
(32) Sholl, D. S.; Asthagiri A.; Power, T. D. *J. Phys. Chem. B* **2001**, *105*, 4771.

(33) Gay, J. G.; Berne, B. J. *J. Chem. Phys.* **1981**, *74*, 3316.
(34) Memmer, R.; Jannsen, F. *J. Chem. Soc., Faraday Trans.* **1998**, *94*, 267.
(35) Memmer, R. *J. Chem. Phys.* **2001**, *114*, 8210.
(36) Steele, W. A. *Surf. Sci.* **1973**, *36*, 317.
(37) Patrykiejew, A.; Sokołowski, S.; Zientarski, T.; Binder K. *J. Chem. Phys.* **1995**, *102*, 8221.
(38) Allan, M. P.; Tildesley, D. J. *Computer Simulation of Liquids*; Clarendon: Oxford, U.K., 1987.
(39) Landau, D. P.; Kinder, K. *A Guide to Monte Carlo Simulation in Statistical Physics*; Cambridge University Press: Cambridge, U.K., 2000.
(40) Patrykiejew, A.; Sokołowski, S.; Sałamacha, L.; Binder, K. *J. Chem. Phys.* **2004**, *120*, 1017.